WWW.IJRPR.COM

International Journal of Research Publication and Reviews

Journal homepage: www.ijrpr.com ISSN 2582-7421

Hybrid Beamforming for High-Performance MIMO Systems: A Comparative Analysis of Zero-Forcing, MMSE and Notch Steering Approaches

P. Poorna Govindu[1], M. Pravalika[2]

[1]*ECE Department, GMRIT, Rajam, AP. poornagovind662@gmail.com*
[2]ECE Department, GMRIT, Rajam, AP. pravallikamamidi32@gmail.com

ABSTRACT –

This paper presents a comparative analysis of three advanced hybrid beamforming and transceiver design techniques for modern communication systems, highlighting their spatial multiplexing and multi-input multi-output (MIMO) capabilities. The first technique utilizes a zero-forcing approach for spatial interference suppression, achieving precise interference cancellation with matrix inversion while enhancing spatial multiplexing performance. The second method introduces a minimum mean-square error (MMSE) hybrid beamforming receiver, offering reconfigurable MIMO operation at 28- and 37-GHz bands, dual-band functionality, >35-dB image rejection, and ~50-dB inter-carrier interference suppression. The third technique implements a notch steering scheme for hybrid beamforming transmitters, leveraging auxiliary-path vector modulators to create deep spatial notches (>35 dB) with minimal main-beam power loss, enabling effective spatial multiplexing and high SINR. This study evaluates the trade-offs and performance benefits of these techniques, offering insights for next-generation wireless communication systems.

1.Introduction

Hybrid beamforming systems are one of the key technologies in next-generation wireless communication, which enables effective interference management while achieving high throughput and efficient spectrum utilization. There are two main architectures for these systems: fully connected (FC) and partially connected (PC). The FC architecture connects every antenna to all RF chains, which offers unparalleled flexibility and performance. This configuration supports robust interference management, high array gain, and precise beamforming control, which is ideal for demanding environments requiring superior performance and energy efficiency. However, the complexity of interconnections grows with the number of antennas, which leads to increased hardware requirements and design challenges. In contrast, PC architectures simplify design by connecting only subsets of antennas to RF chains. This reduces power consumption and hardware complexity but limits performance in interference-prone environments, where multipath propagation can be significant. PC architectures are better suited for resource-constrained systems but fall short in any scenario that demands maximum efficiency and robustness.The cornerstone of spatial multiplexing systems is interference management-the simultaneous transmission of multiple data streams. As the number of

streams increases, the potential for interference increases, with a corresponding threat to the overall system performance. To mitigate this, techniques such as notch steering are used, dynamically changing beamforming weights to cancel interference and enhance the SINR. Notch steering is more important in mmWave systems where large antenna arrays are commonly found, ensuring spatial streams can be separated efficiently. For example, in a four-element receiver array that supports two data streams, notch steering can be achieved by fine-tuning the gain of variable gain amplifiers (VGAs), which enables accurate targeting of each stream. Algorithms such as Minimum Mean-Square Error (MMSE) further enhance this process by dynamically optimizing beamforming weights, achieving better SINR and improving overall system resilience. This calls for proper interference management on the transmitter side also, especially with configurations that involve a uniform linear array, as the sidelobes of the radiation pattern will overlap with some of the main beams from other data streams and contribute to co-channel interference, more critically so with the higher order modulation schemes like quadrature amplitude modulation (QAM).

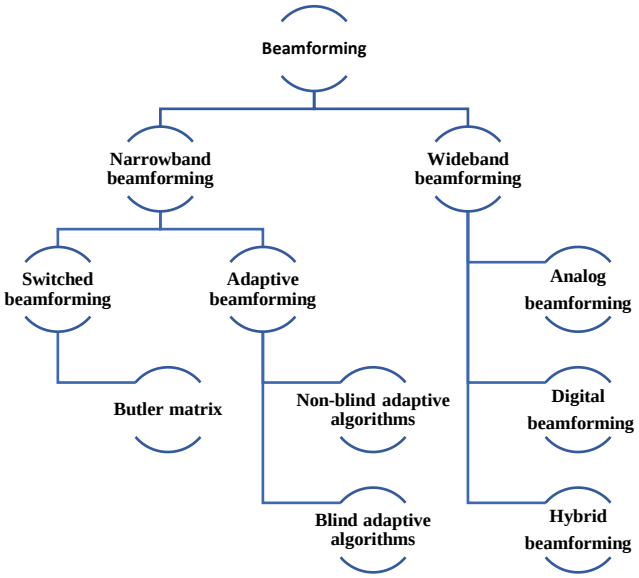

Fig.1.1 Classification of Beamforming techniques.

Increasing the antenna count provides a limited number of sidelobe suppression; an increase from 4 to 128 antennas yields only modest sidelobe improvements of 2 dB. High-performance designs like Dolph–Chebyshev arrays reduce the sidelobes by setting unequal amplitudes among array elements. However, at the same time this affects the efficiency of both a particular element and, thus, a system. For example, for such an antenna to have a -30 dB sidelobe level, some elements need 60% amplitude reduction so that the main-beam power is reduced by 3 dB. Further advancements in interference cancellation rely on sophisticated signal processing algorithms, such as Zero-Forcing (ZF) and MMSE beamforming. ZF cancels interference by applying the inverse of the channel matrix to the beamforming weights but will amplify noise, degrading performance. MMSE strikes a balance between interference and noise minimization, making it more robust in real-world scenarios. When combined with notch steering, these algorithms enable adaptive interference cancellation, ensuring high-quality communication in dynamic environments. As wireless technologies continue to evolve with 5G and terahertz systems, the demand for higher data rates, lower latency, and efficient spectrum utilization increases. Hybrid beamforming, notch steering, and advanced algorithms such as ZF and MMSE will be key enablers in meeting these challenges and will help drive transformative innovations across industries toward a future of global connectivity.

2.1 Zero Forcing

Amplitude and phase tuning make notch steering more flexible, thereby enhancing the interference control. The desired amplitude and phase for an antenna element can be attained in a variety of ways. Of these, the most promising technique is the Zero Forcing technique. Zero Forcing is one of the techniques used by MIMO to minimize interference. It operates by pre-filtering the received signal with the inverse of the channel matrix: interference is nulled, and the desired signal is left isolated. ZF interference suppression is very effective. However, there is a compromise: if the channel matrix is poorly conditioned, ZF will be an amplifier for noise and can degrade signal quality. So interference reduction is balanced by the possibility of noise enhancement. In zero-forcing, the complex weight W is obtained as the pseudo inverse of the channel matrix H by, $\mathbf{W}=(\boldsymbol{H}^{\boldsymbol{H}}\mathbf{H})^{-1}\boldsymbol{H}^{\boldsymbol{H}}$ Here,$(.)^{\boldsymbol{H}}$denotes the Hermitian transpose, and $H = [h_{1,2,3,} \ldots . h_K]$ represents the (N ×K) channel matrix for (K) users. For a line-of-sight (LOS) channel, $\boldsymbol{h_k} = [\mathbf{1}, \boldsymbol{e}^{j\beta_k}, \ldots \ldots, \boldsymbol{e}^{(N-1)j\beta_k}]^{\boldsymbol{T}} \in \mathbf{C}^{(\mathbf{N}\times\mathbf{K})}$ which is the same as the classic beam steering vector of a Uniform Linear Array (ULA). The zero-forcing approach involves a matrix multiplication and inversion. While the complex weight W can be implemented at the frontend of the transceiver using VGA and PS, the computation of W can only be performed in the digital backend. Computation in the digital backend might be relatively power-consuming and also incur latency.

Parameter	**Zero Forcing**
Technology	90nm CMOS
Package	1156-pin ceramic flip-chip BGA
Supply voltage	1.2V, 2.5V
Max data rate	10.3125 Gb/s
# of channels	4
Tx FFE	2 or 3 tap

Rx FFE Control scheme	Analog S-ZF
RX DFE Speculative Control scheme	1-tap Full (1-tap) Heuristics
Total insertion loss at $f_s/2$	15.7-35.8 dB
Area TX per channel RX per channel EQ adaptive	Total 3.03 mm^2 0.166 mm^2 0.214 mm^2 0.065 mm^2
Power dissipation TX per channel RX per channel	 153 mW 107 mW

Table 2.1.1 Specifications of Zero-Forcing system.

2.2.1 Minimum Mean Square Error (MMSE) Beam Adaptation:

The proposed reconfigurable hybrid beamforming receiver operates at 28 GHz and 37 GHz, supporting advanced multi-standard MIMO communication and carrier aggregation (CA). It employs a fully connected Cartesian combining hybrid beamforming (FC-HBF) structure, enhancing its capabilities for 5G and beyond. At the system's core is a novel time-multiplexed least mean square (TM-LMS) mechanism that implements MMSE beam adaptation. This mechanism dynamically optimizes beamforming weights in real-time, improving signal fidelity and robustness in dynamic environments. The receiver architecture integrates FC-HBF for different operational modes, including MIMO dual streams at 28 GHz or 37 GHz, and CA modes for single-stream operation across both frequencies. A Cartesian-combining RF-domain complex-weighting structure, incorporating dual-band active combiners with coupled-resonator-based gain stages, enables high-fidelity signal processing across widely separated frequency bands. This ensures excellent signal quality while supporting flexible and efficient operation.

The receiver features dual-band low-noise amplifiers (LNAs) and current-mode active combiners optimized for 28 GHz and 37 GHz bands. The LNAs employ coupled-resonator loads to provide high gain and a low-noise figure. Current-mode combiners merge wideband signals with minimal loss. Signal down-conversion is facilitated by two-stage heterodyne mixers, offering image-rejection (IR) capabilities. A new quadrature error detection and correction mechanism reduces signal artifacts, ensuring high signal integrity and enhanced performance in multi-band operations.

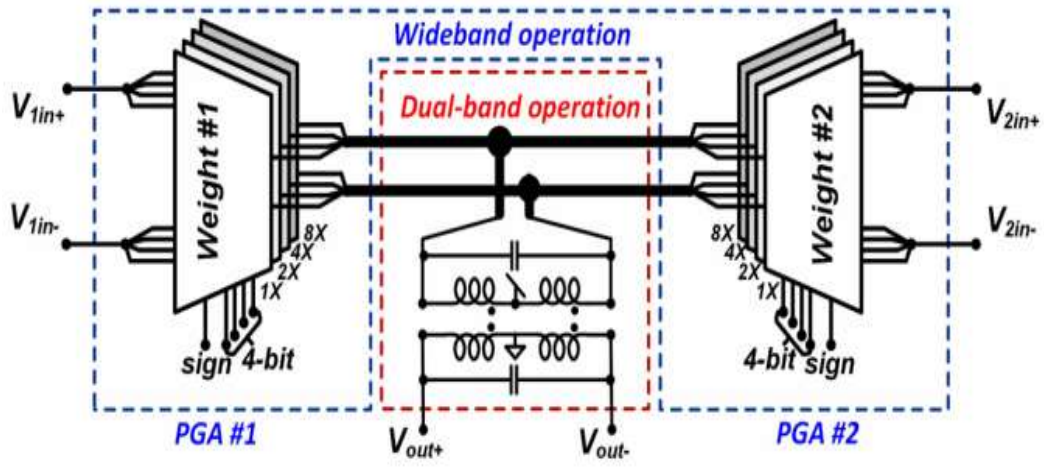

Fig.2.2.1.1Dual-band current-mode active combiner with programmable transconductor to realize dual-band complex weighting.[1].

The Fig.2.2.1.1 shows a dual-band current-mode active combiner with programmable transconductors for dual-band complex weighting. Here, this structure falls within a system focused on enabling wideband and dual-band operations in a reconfigurable beamforming receiver. The proposed receiver architecture enables concurrent dual-band operation, processing signals at 28 GHz and 37 GHz simultaneously. It features adjustable transconductances

for precise phase shifting and amplification of input signals, utilizing programmable weights for complex signal processing. The combiner architecture integrates outputs from antenna paths in the current domain, enhancing performance for dual-band operation. Phase and amplitude control ensure stable beamforming across different frequency bands, while programmable gain amplifiers (PGAs) adjust the gain of combined signals before further processing. The receiver employs a concurrent dual-band front-end with image-reject downconversion in two stages. This design efficiently processes signals from two independent bands while rejecting interference. The per-element complex weighting mechanism improves beamforming precision and minimizes cross-band interference, making the architecture ideal for advanced communication systems. MMSE beam adaptation, powered by a TM-LMS algorithm, optimizes beam patterns in real-time under fluctuating conditions. The system supports main lobe adaptation and adaptive null-steering, enhancing interference mitigation in multi-user MIMO setups. A fabricated four-element prototype on a 65-nm CMOS process demonstrated impressive performance: conversion gains of 33 dB at 28 GHz and 26.5 dB at 37 GHz, noise figures of 5.7 dB and 8.5 dB respectively, and an image rejection ratio exceeding 35 dB. Accurate beam steering and over 25 dB peak-to-null interference rejection validate its capability for simultaneous dual-band beamforming, ensuring high signal clarity and efficiency.

2.2.2 Beamforming without null-steering

MIMO beam patterns at 28- and 37-GHz band measured with array element pairs (1, 2), (2, 3), and (3, 4). The stream 1 is steered toward 0° angle, and stream 2 is steered toward −30° angle with normal.[1].

The architecture described is good for carrier aggregation, with inter-carrier interference rejection of over 50 dB, and therefore very efficient for multi-standard communications. The receiver also shows good accuracy in beam steering and nulling under test conditions, which validates the FC-HBF design for real-world applications requiring reliable multi-stream and dual-band operation. Timing diagrams of the weight update processes in DS-TM-LMS and MS-TM-LMS algorithms for a four-element adaptive beamforming system are shown. In the DS-TM-LMS algorithm, the data clock controls data sampling and the adaptation clock controls weight updates. At each data clock cycle, the data inputs are sequentially processed: x1,k, x2,k, etc. The weights W1,k, W2,k, etc. are updated on the negative edge of the adaptation clock. It cycles through all elements and does one iteration per sequence. In the MS-TM-LMS algorithm, weights for multiple streams are updated simultaneously.

Parameter	MMSE
Single Element	
Technology	65-nm CMOS
Freq. (GHz)	27-29.75
Power(mW)	0.46
iP_{1dB} (dBm)	-30
NF_{min}(dB)	<-10
S_{11} (dB)	5.7
Area$(mm)^2$	52.5
Gain (dB)	33

Table 2.2.1 Specifications of Zero-Forcing system.

The weights for different streams are updated alternately on the positive and negative edges of the adaptation clock, thereby enhancing the processing speed. Output samples are collected on the negative edge, ensuring efficient and timely adaptation.

Both algorithms coordinate data input updates and weight update through clock signals for the accurate and timely adaptation. The MS-TM-LMS algorithm is quite promising because of its ability to make parallel processing possible in multistream systems. Comparison between performance of single-element and phased array configurations shows that the system is very efficient for adaptive beamforming in different scenarios.

2.3.1 Notch Steering using Vector Modulators

High-performance mmWave antenna arrays, especially in systems using higher-order modulation like 64-QAM, require notch steering. Modern beamformers use VGAs and PSs to control the amplitude and phase of antenna elements. The finite tuning range and resolution of these components limit the effectiveness of spatial notches used to suppress interference. For example, with a 6-bit PS and a VGA with a 10 dB tuning range, the achievable notch depth is limited, leading to only moderate interference suppression. Therefore, an innovative technique that utilized vector-modulated, auxiliary-path approaches is now proposed to enhance the earlier limitations. Through this strategy, a fundamental beam, as well as an auxiliary beam, which cancels unwanted signals from interference patterns by creating an additional phase shift of 180° into the interference patterns of the arrays, is implemented for sharpening of spatial nulls and enhancements in interference suppressing.

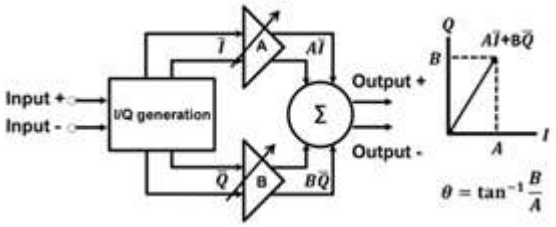

Fig.2.3.1 I/Q vector modulator based phase rotator architecture

The auxiliary-path configuration has several advantages: enhanced SINR, improved performance, and increased data rates. However, the resolution of VGAs and PSs continues to be a significant performance optimization challenge. It may improve notch depth and interference rejection capability but at the cost of higher hardware complexity, increased power consumption, and additional costs.

The auxiliary-path vector modulation technique solves the problem by providing accurate interference control without requiring significant hardware upgradation, which makes it suitable for next-generation mmWave communication systems. The interaction of the array factors (AFs) of the auxiliary and main beams in the far-field region produces the desired beamforming effect. The overall array factor for an N-element linear array can be expressed as:

$$AF_{tot} = \sum_{n=0}^{N} AF_{main} + \xi \sum_{n=0}^{N} AF_{Aux}$$

where ξ represents the amplitude scaling factor of the auxiliary beam, and α accounts for the phase gradient of the auxiliary path. The notch direction is denoted by θ. By properly adjusting these parameters, optimal interference cancellation can be achieved, where $AF_{tot}(\theta) = 0$ effectively nullifying unwanted signals in the desired direction.

2.3.2 Beam Steering and Notch Formation Mechanism

The key mechanisms for millimeter-wave (mmWave) antenna arrays are beam steering and notch formation, playing the important role of enhanced reliability in communications, in high-data-rate systems especially. These mechanisms optimize the signal integrity through steering it into the required direction as well as through notch suppression mechanisms in interference conditions, as highly packed signal environments combined with high-order modulation schemes of up to 64-QAM require very high data throughput.

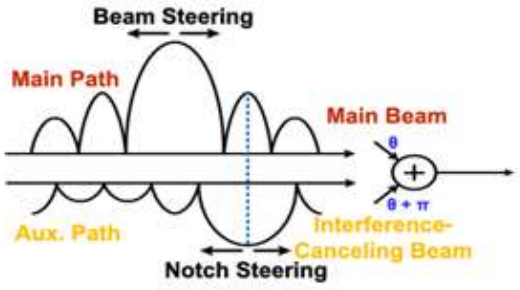

Fig.2.3.2 interference cancellation by creating auxiliary paths [4]

Coordinated manipulation of the antenna elements achieves beam steering in a traditional manner, making use of the phase shifters placed along the main path of the signal. In fact, by the proper variation of the phases of individual antenna elements, energy will be radiated towards a selected angle, making it produce a high gain in a main beam direction. By this process, the power will be highly concentrated toward a target direction; therefore, the SNR and also the communication will be enhanced. Besides beam steering, interference cancellation is an important feature to ensure reliable communication, especially in congested frequency bands. To mitigate interference, an auxiliary path is introduced along with the main beam. The auxiliary beam is designed to have the same amplitude as the main beam but with a 180° phase shift in the direction of interference. If both beams interact in the far-field region, then unwanted signals coming from the interference direction are cancelled due to the destructive interference coming from the auxiliary beam. At the same time, the constructive interference of the main beam ensures that it will not be affected by interference. This results in improved interference rejection in the system, thereby keeping the main signal intact. The effective integration of both beam steering and notch formation will allow for achieving excellent performance in interference-laden environments for mmWave communication systems. Such dual methodology is particularly important for applications under sensitive conditions that may ensure robust, high-speed data transmission and ensure continued communication reliability in future generations of wireless networks.

Section-3

Reference	**JSSC'22[5]**	**JSSC'22[6]**	**Notch Steering by auxiliary path**	**JSSC'21[7]**
Beamforming Architecture	Hybrid(FC)	Analog	Hybrid (FC)	Analog
Frequency (GHz)	28/37	24-30	29	28
Modulation Bandwidth (MHz)	250	400	400	400
Modulation Type	16-QAM	64-QAM OFDM	64-QAM	64-QAM OFDM
Number of Data Streams	2 (Same Polarization)	2 (Dual Polarization)	2 (Same Polarization)	2 (Dual Polarization)
Notch Steering	Yes Notch Depth>25	No	Yes Notch Depth>35	No
RMS Gain Error(db)	N/A	±0.5	0.28	0.12
P_{sat} (dbm)/Element	15.5	17	20.4	16.1
Phase Resolution(º)	N/A	4-5.6	3.0	N/A
Chip Area(mm)^2	12.65	36.96	7.5	16
RMS Phase Error(º)	N/A	1.35	0.96	0.4
Technology	65-nm CMOS	130-nm SiGe BICMOS	45-nm CMOS SOI	65-nm CMOS

Table 3.1 Comparison of Beamforming Techniques

3.1 Insights and Practical Implications

The figures and analysis here demonstrate the significant role of notch steering in robust interference management for mmWave communication systems. Notch steering is a paradigm shift in beamforming technology that creates deep spatial notches in one or several directions to suppress unwanted signals. The main and auxiliary-path beams combined give this method precise spatial control while keeping the integrity of the main communication channel and at the same time effectively mitigating interference. This capability is important, especially for high-order modulation schemes, such as 64-QAM, which require a high signal-to-interference-plus-noise ratio (SINR) for reliable demodulation. Single-notch configurations show their effectiveness in canceling interference from a specific direction, whereas dual-notch configurations extend this flexibility to tackle more complex interference scenarios. The performance obtained indicates the adaptability of notch steering, which is critical in modern, dynamic interference environments. The implementation of these techniques, however, comes with challenges. VGAs and PSs have finite resolutions, which inherently limit the depth and accuracy of spatial notches. Increasing the resolution of these components can enhance performance but comes with greater hardware complexity, higher power consumption, and increased costs. The auxiliary-path vector modulation technique promises to solve these problems with efficient beamforming and reliable interference suppression, scalable implementation. This has the potential to revolutionize mmWave communication systems by offering higher reliability, enhanced data rates, and improved communication quality in next-generation wireless networks.

4. Conclusion

The comparative study of zero-forcing, MMSE, and notch steering techniques reveals that each hybrid beamforming technique is uniquely suited with its strengths and trade-offs for MIMO-based wireless communication. Zero-forcing excels in interference cancellation and spatial multiplexing but is computationally intensive. MMSE achieves a balance of adaptability and interference suppression, with the suitability for reconfigurable MIMO systems. It is interference-heavy, deep spatial notches with the least power loss in a low-latency scenario. This emphasis points toward suitability for particular applications in both designs, giving guidelines on how hybrid beamforming architectures may be used for designing next-generation systems. In particular, notch steering will become a game changer because of the prospect of more advanced reliability and much higher data rates combined with greater quality communication over very new and fast-changing wireless network scenarios.

References

[1] Mondal, Susnata, and Jeyanandh Paramesh. "A reconfigurable 28-/37-GHz MMSE-adaptive hybrid-beamforming receiver for carrier aggregation and multi-standard MIMO communication." *IEEE Journal of Solid-State Circuits* 54.5 (2019): 1391-1406.

[2] Hidaka, Yasuo, et al. "A 4-channel 1.25–10.3 Gb/s backplane transceiver macro with 35 dB equalizer and sign-based zero-forcing adaptive control." *IEEE Journal of Solid-State Circuits* 44.12 (2009): 3547-3559.

[3] Hu, Yaolong, Xiaohan Zhang, and Taiyun Chi. "A 28-GHz Hybrid Beamforming Transmitter With Spatial Notch Steering Enabling Concurrent Dual Data Streams for 5G MIMO Applications." *IEEE Journal of Solid-State Circuits* (2024).

[4] Hu, Yaolong, Xiaohan Zhang, and Taiyun Chi. "A 28GHz Hybrid-Beamforming Transmitter Array Supporting Concurrent Dual Data Steams and Spatial Notch Steering for 5G MIMO." *2021 IEEE Custom Integrated Circuits Conference (CICC)*. IEEE, 2021.

[5] Steyskal, Hans, R. A. Shore, and R. Haupt. "Methods for null control and their effects on the radiation pattern." *IEEE Transactions on Antennas and Propagation* 34.3 (1986): 404-409.

[6] Sadhu, Bodhisatwa, et al. "A 24–30-GHz 256-element dual-polarized 5G phased array using fast on-chip beam calculators and magnetoelectric dipole antennas." *IEEE Journal of Solid-State Circuits* 57.12 (2022): 3599-3616.

[7] Pang, Jian, et al. "A CMOS dual-polarized phased-array beamformer utilizing cross-polarization leakage cancellation for 5G MIMO systems." *IEEE Journal of Solid-State Circuits* 56.4 (2021): 1310-1326.

[8] K. Kibaroglu, M. Sayginer, T. Phelps, and G. M. Rebeiz, "A 64-element 28-GHz phased-array transceiver with 52-dBm EIRP and 8–12-Gb/s 5G link at 300 meters without any calibration," IEEE Trans. Microw. Theory Techn., vol. 66, no. 12, pp. 5796–5811, Dec. 2018.

[9] J. Park, S. Lee, J. Chun, L. Jeon, and S. Hong, "A 28-GHz four channel beamforming front-end IC with dual-vector variable gain phase shifters for 64-element phased array antenna module," IEEE J. Solid State Circuits, vol. 58, no. 4, pp. 1142–1159, Apr. 2023.

[10] Y. Yi et al., "A 24–29.5-GHz highly linear phased-array transceiver front-end in 65-nm CMOS supporting 800-MHz 64-QAM and 400-MHz 256-QAM for 5G new radio," IEEE J. Solid-State Circuits, vol. 57, no. 9, pp. 2702–2718, Sep. 2022.

[11] K. Kibaroglu, M. Sayginer, and G. M. Rebeiz, "A low-cost scalable 32-element 28-GHz phased array transceiver for 5G communication links based on a 2×2 beamformer flip-chip unit cell," *IEEE J. Solid-State Circuits*, vol. 53, no. 5, pp. 1260–1274, May 2018.

[12] T. Chi, J. Park, S. Li, and H. Wang, "A millimeter-wave polarization division-duplex transceiver front-end with an on-chip multifeed self-interference-canceling antenna and an all-passive reconfigurable canceller," *IEEE J. Solid-State Circuits*, vol. 53, no. 12, pp. 3628–3639, Dec. 2018.

[13] J. Pang et al., "A CMOS dual-polarized phased-array beamformer utilizing cross-polarization leakage cancellation for 5G MIMO systems," *IEEE J. Solid-State Circuits*, vol. 56, no. 4, pp. 1310–1326, Apr. 2021.

[14] T. Chi, J. S. Park, S. Li, and H. Wang, "A 64 GHz full-duplex transceiver front-end with an on-chip multifeed self-interference-canceling antenna and an all-passive canceler supporting 4 Gb/s modulation in one antenna footprint," in *IEEE Int. Solid-State Circuits Conf. (ISSCC) Dig. Tech. Papers*, Feb. 2018, pp. 76–78.

[15] J. S. Park and H. Wang, "A K-band 5-bit digital linear phase rotator with folded transformer based ultra-compact quadrature generation," in *Proc. IEEE Radio Freq. Integr. Circuits Symp.*, Jun. 2014, pp. 75–78

[16] S. Dong et al., "A 140 GHz RF beamforming phased-array receiver supporting >20 dB IRR with 8 GHz channel bandwidth at low IF in 22 nm FDSOI CMOS," in *Proc. IEEE Radio Freq. Integr. Circuits Symp. (RFIC)*, Jun. 2023, pp. 293–296.

[17] X. Zhang, S. Li, D. Huang, and T. Chi, "A millimeter-wave three-way Doherty power amplifier for 5G NR OFDM," *IEEE J. Solid-State Circuits*, vol. 58, no. 5, pp. 1256–1270, May 2023.

[18] Y. Yoon et al., "A highly linear 28GHz 16-element phased-array receiver with wide gain control for 5G NR application," in Proc. IEEE Radio Freq. Integr. Circuits Symp. (RFIC), Jun. 2019, pp. 287–290.